GEOPHYSICAL RESEARCH LETTERS, VOL. 24, NO.8, PAGES 983-986, APRIL 15, 1997

Solar wind-magnetosphere coupling during an isolated substorm event: A multispacecraft ISTP study

T. I. Pulkkinen[1,2], D. N. Baker[1], N. E. Turner[1], H. J. Singer[3], L. A. Frank[4], J. B. Sigwarth[4], J. Scudder[4], R. Anderson[4], S. Kokubun[5], R. Nakamura[5], T. Mukai[6], J. B. Blake[7], C. T. Russell[8], H. Kawano[8], F. Mozer[9], J. A. Slavin[10]

Abstract. Multispacecraft data from the upstream solar wind, polar cusp, and inner magnetotail are used to show that the polar ionosphere responds within a few minutes to a southward IMF turning, whereas the inner tail signatures are visible within ten min from the southward turning. Comparison of two subsequent substorm onsets, one during southward and the other during northward IMF, demonstrates the dependence of the expansion phase characteristics on the external driving conditions. Both onsets are shown to have initiated in the midtail, with signatures in the inner tail and auroral oval following a few minutes later.

Introduction

Exploration of the Earth's space environment has revealed a dynamic system of interacting plasmas, magnetic fields and electrical currents. The near-Earth environment has traditionally been studied as a system of independent components – the interplanetary region, the magnetosphere, the ionosphere, and the upper atmosphere. A key objective of the International Solar Terrestrial Physics program is to understand how the individual parts of the coupled, time-dependent geospace systems work together (see, e.g., Acuña et al., [1995] and associated references for the instrumentation used here).

Magnetospheric substorms represent the basic form of solar wind–magnetosphere interaction. A particularly well-observed substorm event is studied here using a multitude of satellites in the solar wind and magnetosphere together with ground-based observations. Observations in the solar wind and in the vicinity of the cusp are used to demonstrate the rapid time scale in which the growth phase initiates. Comparison of two substorm onsets under different IMF conditions shows the dependence of the substorm expansion phase characteristics on the global conditions. Auroral images and ground magnetograms are used to deduce the substorm onset location.

[1]Lab. for Atmospheric and Space Physics, University of Colorado, Boulder, CO
[2]Permanently at: Finnish Meteorological Institute, Helsinki, Finland
[3]NOAA Space Environment Center, Boulder, CO
[4]Dept. of Physics and Astronomy, University of Iowa, Iowa City, IA
[5]Solar Terrestrial Environment Laboratory, Nagoya University, Toyokawa, Japan
[6]Institute of Space and Astronautical Science, Sagamihara, Japan
[7]The Aerospace Corporation, Los Angeles, CA
[8]Institute of Geophysics and Planetary Physics, University of California, Los Angeles, CA
[9]Space Science Lab., University of California, Berkeley, CA
[10]NASA Goddard Space Flight Center, Greenbelt, MD

Paper number 97GL00816.
0094-8534/97/97GL-00816$05.00

Observations

Solar wind – magnetosphere coupling

Fig. 1a shows the upstream IMF B_Z measured by IMP-8 and WIND. During this time period, B_Y was continuously negative at about −5nT, and B_X changed sign shortly after the B_Z southward turning before 0600 UT.

IMF and solar wind speed data during 0530–0550 UT from WIND and IMP-8 suggest that the southward turning recorded at WIND at 0537 UT (0543 UT at IMP-8) arrived at the magnetopause at ~0548 UT. Similarly, the northward turning recorded by WIND at about 0652 UT arrived at the magnetopause between 0705 UT (first turning) and 0707 UT (second turning leading to continuously positive B_Z). A reduction of the flow speed at the bow shock can cause up to ~3 min delay to this timing [Spreiter and Stahara, 1980].

POLAR was near local noon moving poleward through the dayside auroral zone after 0500 UT. The EFI electric field instrument showed significant enhancement of fluctuations in the DC electric field commencing at ~0548 UT (Fig. 1a). At the same time, the electric component of the PWI wave instrument also detected increased power at low frequencies (<100 Hz, Fig. 1b); at that time there was very little power in the magnetic wave component (not shown). Ion data from HYDRA showed a simultaneous increase in ion fluxes (~0.1–10 keV). These signatures could indicate a magnetospheric response to the southward IMF turning (equatorward motion of the cusp).

The POLAR magnetic field data became slightly more noisy at 0548 UT (Fig. 1a). During 0555–0606 UT the satellite entered a region of depressed field magnitude, the polar cusp. During this period, the PWI

wave intensity was largest, and the medium resolution EFI electric field data showed spikes at a few–Hz frequency up to 50 mV/m. This is also the time of largest fluxes in the HYDRA ion data. At 0558 UT, there was an abrupt change in the ion dispersion, which is indicative of an IMF southward turning. The later arrival of this signature than the propagated solar wind data can be attributed to the time it takes the reconnected field lines to convect over the satellite location [Lockwood, 1995].

After 0605 UT, the low level of energetic particle fluxes (not shown) indicated that the satellite was on open field lines. The ion signatures (with decreasing mean energy and flux level) and wave activity persisted throughout the period of southward IMF until a few minutes after 0700 UT. This suggests that the IMF also influences the dynamics in the dayside polar cap.

Fig. 2 shows data from the CANOPUS and Greenland magnetometer chains. The eastward and westward electrojets started to enhance a few minutes before 0600 UT, very shortly after the southward IMF turning. When mapped to the magnetotail, this corresponds to convection enhancement at 20–30 R_E in the tail.

Spacecraft in the inner magnetotail recorded growth phase signatures at about 0600 UT, <10 min after the southward IMF turning: Fig. 3 shows the B_Z depression at geostationary orbit (field line stretching), and the B_X increase at GEOTAIL (current sheet thinning and intensification). The dawn-to-dusk convection electric field at GEOTAIL (computed from $\mathbf{E} = -\mathbf{v} \times \mathbf{B}$) increased from 0600 UT onward, from ~0.15 to 0.35 mV/m during a 40 min before strong fluctuations related to the current disruption at GEOTAIL began.

Substorm evolution

The ground-based observations (Fig. 2) show two substorm onsets, one at 0623 UT at GILL (63.9° Mlat and 23.7 MLT), and a subsequent one at 0706 UT at FSMI (66.6° Mlat, 22.1 MLT).

Although the ground signatures of both onsets are quite similar (~300 nT negative bay), their global consequences were different. Fig. 4 shows global auroral images taken by the POLAR VIS imager at the peak of the expansions of the two onsets and during the recovery phase of the latter onset. The first brightening was localized and did not cause much change in the polar cap size or the oval width. On the other hand, the second onset led to a major expansion, formation of a high-latitude arc system (double oval) in the morning sector, and a greatly reduced polar cap size.

In the magnetotail, the first onset was detected 3 min after the ground onset, at ~0626 UT by GOES-8 (a slight field dipolarization) and the LANL energetic particle detectors onboard s/c 1990-095 (dispersed electron signatures at ~0500 MLT, Fig. 3). GEOTAIL measured a small B_Z increase at about the same time, and B_Z decreased at GOES-9 in the evening sector, suggesting that the spacecraft was still outside the substorm current wedge.

At 0655 UT, the field at GOES-9 dipolarized, and the LANL instrument recorded another dispersed ion signature. This dipolarization event had no observable ground signatures, and did not cause changes in the auroral activity. The field stretching continued, as both GOES-8 and GOES-9 measured decreasing B_Z values. The field dipolarizations associated with the second onset occurred at about 0712 UT at GOES-9 and at about 0722 UT at GOES-8.

The substorm onset signatures at GEOTAIL, located only few R_E away from GOES-8, showed quite different behavior: The magnetic field dipolarization occurred in four distinct bursts, at 0642, 0652, 0708, and 0727 UT. Each of these was associated with a moderate flow burst in the X and Y direction (~200 km/s) and B_Y signatures consistent with a field-aligned current toward the ionosphere poleward of the satellite location. These dipolarizations showed no signatures in the available ground magnetograms.

Field-aligned currents (B_Y disturbances) were recorded by both GOES-8 and GOES-9 during the two onsets at 0623 and 0706 UT; somewhat earlier at GOES-8 (morning sector) than at GOES-9 (evening sector). The B_Y signatures at GOES-8 were seen during both onsets a few minutes before other signatures of the onset either on the ground or in the auroral images.

Discussion

The multisatellite data clearly show that the high-latitude ionospheric current systems responded within a few minutes to the southward turning of the IMF; the nightside magnetosphere (<10 R_E) showed growth-

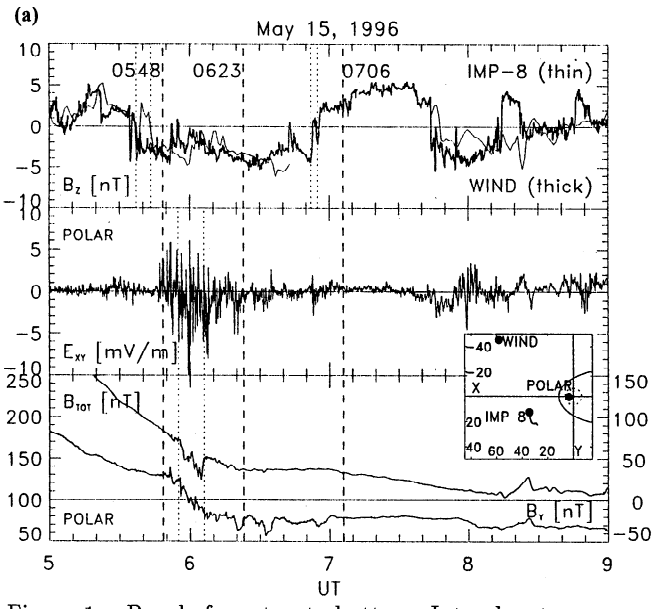

Figure 1a. Panels from top to bottom: Interplanetary magnetic field B_Z from WIND (heavy line) and IMP 8 (thin line) in GSM coordinates. Electric field from POLAR/EFI. E_{XY} is a spin fit (6 s) component in the spin plane; for this event E_{XY} was in the generally antisunward direction. Magnetic field from POLAR in GSM coordinates. The insert shows the satellite positions in a GSM $X - Y$ plane projection.

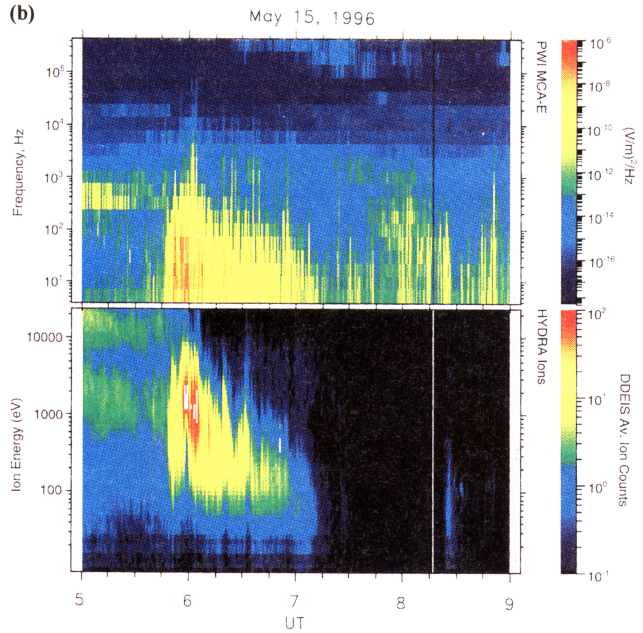

Figure 1b. Electric component of the wave frequency-time spectrogram from POLAR/PWI. Ion and electron energy-time spectrograms from POLAR/HYDRA.

phase features <10 min after the IMF turning. Comparison of multipoint tail and ground data indicate that the inner tail magnetic field dipolarizations are not accurate indicators of substorm onset times as they may be significantly delayed or show variable behavior even at two relatively close locations.

The solar wind observations were used to examine whether the two substorm onsets were internally or externally triggered [Rostoker, 1983]: The first substorm onset (0623 UT) was not associated with any apparent changes in the solar wind parameters, but rather was the result of an internal instability in the near-midnight magnetotail. The second onset (0706 UT) occurred close to the IMF northward turning, suggesting the substorm may have been externally triggered.

The two expansion phases were very different: The first substorm remained localized and did not expand much poleward. The mapped locations of the satellites

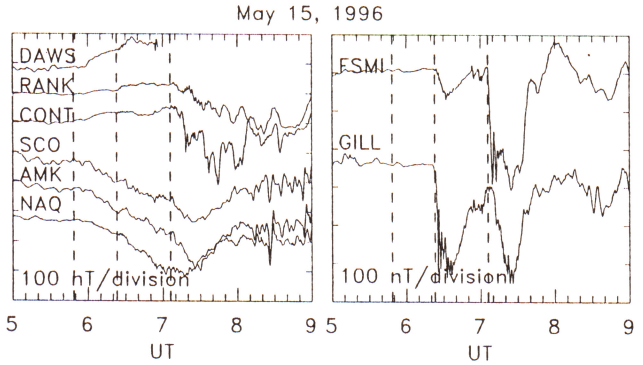

Figure 2. X component of ground magnetic field from magnetometers from Canada and Greenland. Station locations are shown in Figure 4.

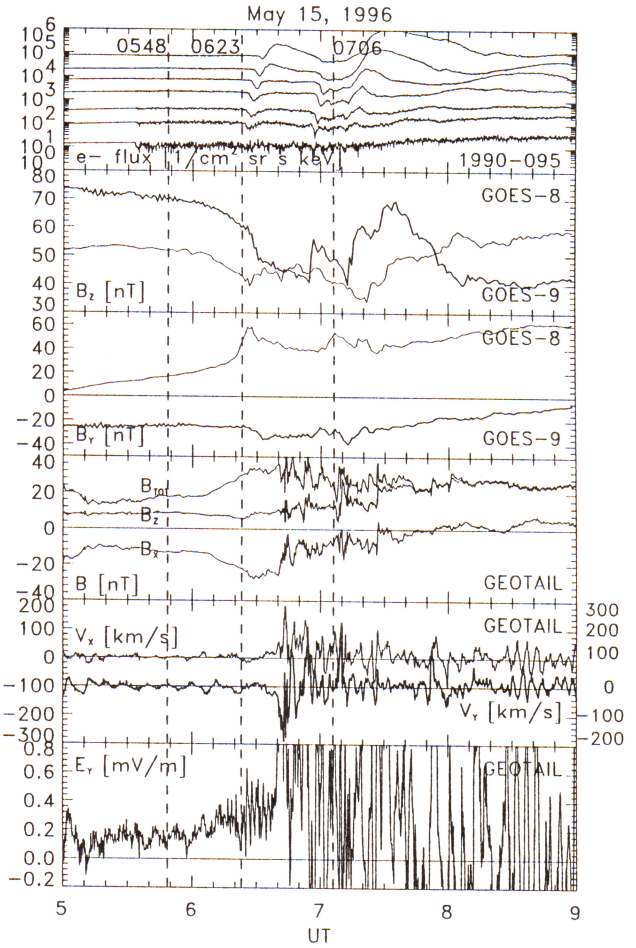

Figure 3. Panels from top to bottom: Electron differential fluxes from s/c 1990-095. Magnetic field B_Z and B_Y from GOES-8 and GOES-9 in GSM coordinates. Magnetic field B_{TOT}, B_Z, and B_X from GEOTAIL. Plasma velocity V_X and V_Y from GEOTAIL/LEP instrument. Electric field from GEOTAIL, computed from $-\mathbf{v} \times \mathbf{B}$. All GEOTAIL data are in GSM coordinates.

show that the current wedge was located between the two GOES satellites, consistent with the high-altitude data. Furthermore, the strongest and first ionospheric negative bay occurred at GILL, poleward of the center of the auroral brightening. This and the tail FAC observations suggest that the disturbance originated in the midtail and initiated before the auroral brightening.

The second onset expanded quite rapidly over a wide range of longitudes, and led to major changes in the auroral oval. Similar to the first onset, the promptness of the FAC-signature at GOES-8, the delay in in field dipolarization at GOES-9, and the location of the ground station showing strongest disturbances poleward of the auroral bulge center suggest that the initial disturbance occurred tailward of geostationary orbit. This would tend to favor substorm onset models such as the NENL model over those assuming a near-Earth initiation of the substorm process.

The very different characteristics of the two expansions may be related to the external conditions: the continuing southward IMF may have stretched the field

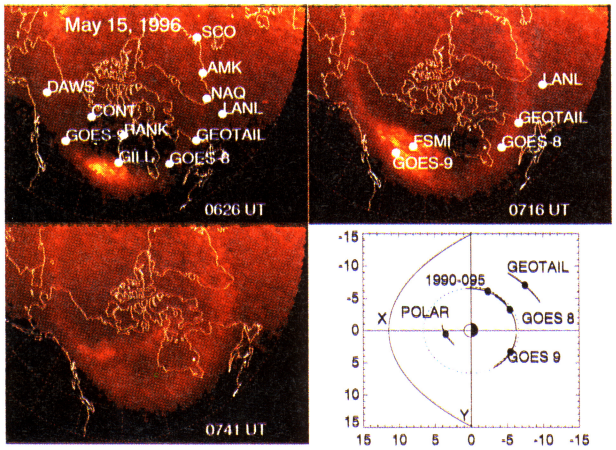

Figure 4. Images taken by the FUV camera of the POLAR/VIS imager. Locations of some ground stations and satellite footprints are shown.

outside the current wedge, and thus slowed the longitudinal expansion of the first event until a further disturbance initiated another activation. This would suggest that substorms during continuously southward IMF consist of multiple intensifications for two reasons: first, the initial expansion cannot expand as rapidly as it would under northward IMF, and secondly the continuous energy input drives the system unstable in a repetitive manner [e.g., Baker et al., 1990].

Acknowledgments. The work of TP was supported by the Finnish Fulbright Commission and by NASA grants. We thank the NSSDC personnel for maintaining the online ISTP key parameter facility. We thank Y. Saito for evaluation of the LEP data and ISAS for GEOTAIL operations, G. Reeves and R. Belian for the LANL energetic particle data, T. Hughes and the Canadian Space Agency for the CANOPUS data, and E. Friis-Christensen for the Greenland magnetometer data. The work at UCLA was supported by NASA grant NAG5-3171. The HYDRA analysis was supported by NASA grant NAG 5 2231 and DARA.

References

Acuña, M. H., et al., The global geospace science program and its investigations, in: C. T. Russell (ed.), *The global geospace mission*, Kluwer Academic Publishers, Dordrecht, the Netherlands, p. 5, 1995.

Baker, D. N., et al., The evolution from weak to strong geomagnetic activity: An interpretation in terms of deterministic chaos, *Geophys. Res. Lett., 17*, 41, 1990.

Lockwood, M., Location and characteristics of the reconenction X line deduced from low-altitude satellite and ground-based observations 1. Theory, *J. Geophys. Res., 100*, 21791, 1995.

Rostoker, G., Dependence of the high-latitude ionospheric fields and plasma characteristics on the properties of the interplanetary plasma, in *High-Latitude Space Plasma Physics*, edited by B. Hultqvist and T. Hagfors, p. 189, Plenum Publ. Co., 1983.

Sibeck, D. G., et al., Solar wind control of the magnetopause shape, location, and motion, *J. Geophys. Res., 96*, 5489, 1991.

Spreiter, J. R., and S. S. Stahara, A new predictive model for determining solar wind-terrestrial planet interactions, *J. Geophys. Res., 85*, 6769, 1980.

R. Anderson, L. A. Frank, J. Scudder, J. B. Sigwarth, Department of Physics and Astronomy, The University of Iowa, Iowa City, IA 52242

D. N. Baker, T. I. Pulkkinen, N. E. Turne, rLaboratory for Atmospheric and Space Physics, University of Colorado, 1234 Innovation Drive, Boulder, CO 80303 (Internet tuija.pulkkinen@lasp.colorado.edu)

J. B. Blake, The Aerospace Corporation, POBox 92957, Los Angeles, CA, 90009

H. Kawano, C. T. Russell, Institute of Geophysics and Planetary Physics, UCLA, Los Angeles, CA 90024-1567

S. Kokubun, R. Nakamura, Solar Terrestrial Environment Laboratory, Nagoya University, Honohara 3-13 Toyokawa, Aich 442, Japan

F. Mozer, Space Science Laboratory, University of California Berkeley, Berkeley, CA 94720

T. Mukai, Institute of Space and Astronautical Science, 3-1-1, Sagamihara, Kanagawa 229, Japan

H. J. Singer, NOAA Space Environment Center, 325 Broadway, Boulder, CO 80303

J. A. Slavin, NASA Goddard Space Flight Center, Greenbelt, MD 20771

(Received October 21, 1996; revised February 28, 1997; accepted March 10, 1997.)